# C30 LANDSLIDE DISPLACEMENT AND ROTATION MONITORING BASED ON PERIODICAL DGNSS MEASUREMENTS AND A COMBINED LOW-COST RTK DGNSS AND MEMS ACCELEROMETER

« BACK TO CONTENT

**Thomas Zieher, Ph.D.; Austrian Research Centre for Forests**
**Innsbruck, AUSTRIA**
Johannes Branke, M.Sc.; Jan Pfeiffer, Ph.D.

## ABSTRACT

Cost-effective monitoring of deep-seated landslides provides vital insights to understand their kinematics and is an important tool for preventing impacts on society. This study presents the results of monitoring campaigns, including the use of low-cost sensors, conducted at the Reissenschuh landslide (Tyrol, Austria) between 2016/05 and 2021/12. Time series of displacement, velocity and the rotational movement component were recorded at 31 observation points based on periodical measurements with the help of a differential global navigation satellite system (DGNSS) and a permanent system combining a low-cost real-time kinematic (RTK) single-frequency DGNSS and a micro-electro-mechanical system (MEMS) accelerometer. Rotational movement components derived from both monitoring campaigns are analysed and interpreted in terms of the landslide's kinematics. The results show that the implemented low-cost system provides valuable insights into the landslide's temporal dynamics.

## INTRODUCTION

In mountain regions worldwide, landslides have severe impacts on society, including damage to property, economic loss and casualties (Petley 2012, Haque et al. 2019). It is therefore vital to monitor their activity to prevent disasters. Particularly slowly moving deep-seated gravitational slope deformations (DSGSDs), potentially endangering settlements, must be continuously monitored. Various measurement techniques are used to quantify landslide displacement over time at characteristic points, along profile lines or area-wide. For monitoring landslide displacements at selected points, a DGNSS is a cost-efficient monitoring technique, offering a measurement precision typically in the order of sub-centimetre to centimetre level (Gili et al. 2000, Teunissen & Montenbruck 2017). However, state-of-the-art equipment required for continuously operating DGNSS is typically expensive, also considering costs for implementation and maintenance. Furthermore, on active landslides it is risky to expose the devices to typically harsh environmental conditions and secondary geomorphological processes (e.g. rock fall, debris flows, snow avalanches) which could destroy the installed monitoring system (Biagi et al. 2016, Malet et al. 2002). In such cases, low-cost systems potentially are cost-efficient solutions for obtaining the required monitoring data without risking to lose costly equipment. In this light, previous studies focussed on assessing the performance of low-cost DGNSSs for displacement monitoring under controlled conditions (e.g. Biagi et al. 2016, Hodgson 2020, Lapadat et al. 2021) and on active, slowly moving landslides (e.g. Malet et al. 2002, Heunecke et al. 2011, Šegina et al. 2020). Furthermore, the combination of a low-cost DGNSS and a MEMS (micro-electro-mechanical systems) accelerometer have been tested for monitoring abrupt (e.g. Tu et al. 2013) and slow ground motion (e.g. Cina et al. 2019).

This study presents monitoring results of a highly active DSGSD in Tyrol (Austria), including periodically conducted DGNSS measurements since 2016/05 and continuous time series of a low-cost station combining an RTK-DGNSS and a MEMS accelerometer deployed in 2020/11. The five years of periodical DGNSS monitoring included observation points where two survey nails were installed on large blocks. The obtained time series allow computing the differential displacement per block, providing insight into the 2D rotational movement component. At the permanently installed station, sub-daily positional measurements are conducted and the tilt angle is continuously monitored with the help of an accelerometer. The results of the individual monitoring campaigns are integrated and compared, considering the respective measurement uncertainty.

## STUDY AREA

The Reissenschuh landslide is part of a deep-seated gravitational slope deformation located in the Schmirn valley (Tyrol, Austria; Fig. 1a,b). It covers an area of about 0.35 km² on a south-east facing slope between 1600 and 2200 m. The Reissenschuh landslide is a rotational rock slide turning into an earth slide in its lower part. It is located entirely within the penninic units of the Tauern-window. Meta-carbonates (Bündner Schiefer), such as calcareous mica schists, calcareous phyllites and calcareous-free phyllites are among the most common rocks within the study area (Rockenschaub et al. 2003). A distinct change from graphite bearing and finely foliated black phyllites in the lying and calcareous Bündner Schiefer in the hanging is exposed right along the scarp of the active landslide. The schistosity dips with approximately 30° towards N. Intense isoclinal folding and multiple sets of majoritarian sub-vertical joints frame the structural appearance at surrounding outcrops. The landslide's surface is covered by European larch (Larix decidua Mill.) forests and shrubs at lower parts, while above the forest line alpine grassland and rock outcrops dominate.

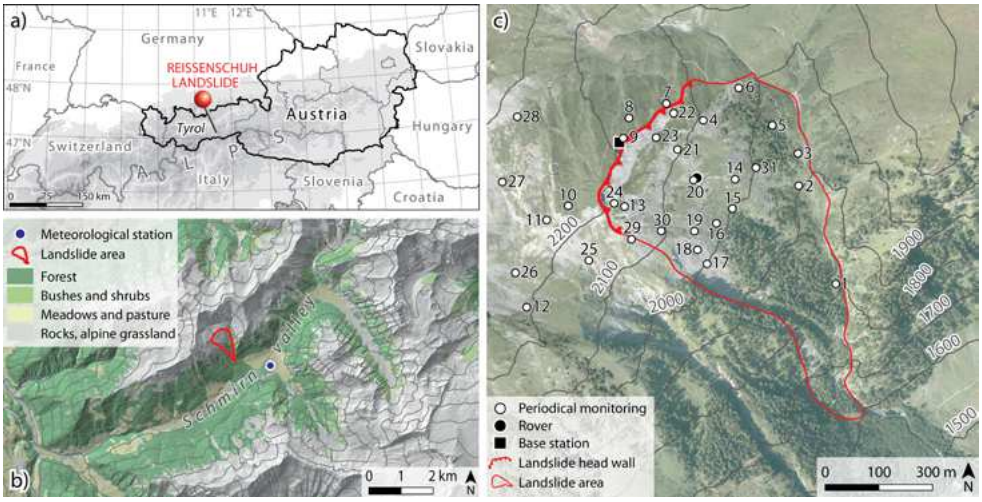


*Figure 1: Location of the Reissenschuh landslide in the province of Tyrol (Austria) (a), overview of the Schmirn valley (b) and detailed view of the landslide and the locations of the installed observation points of the periodical DGNSS monitoring (c). Data source (shaded relief, land cover, orthophoto): Federal state of Tyrol, Division of Geoinformation.*

## METHODS

Since May 2016, the Reissenschuh landslide has been monitored by periodic DGNSS measurements aiming at assessing the spatial pattern of mean landslide displacement and velocity. One goal was to validate the area-wide surface displacement of the deep-seated landslide derived from 3D point cloud analyses based on multitemporal terrestrial laser scanning (Pfeiffer et al. 2018). For that, the position of selected observation points covering the active landslide area and its surrounding were repeatedly measured using a DGNSS (Trimble Geo7X and Zephyr 2 antenna, dual-frequency device). In total, 31 observation points were implemented successively by installing at least one survey mark on top of large blocks and boulders (Fig. 1c, Fig. 2d-i). One survey mark was installed if the block is embedded and supported by the matrix. Two marks were installed on blocks travelling on top of the surface, allowing to detect a 2D rotational movement component. In total, 46 survey marks were installed at the 31 observation points. Almost all of the observation points are located above the forest line to prevent multipath effects in high vegetation. For the measurements, the antenna was put on a 2.0 m pole with a level and fixed in an upright position with a tripod. Due to the lack of GSM (Global System for Mobile Communications) coverage at all the observation points, uncorrected data were acquired and corrected in a post processing step (software Trimble Pathfinder Office V5.85), applying correction data recorded at the closest permanent station located about 16 km south in Sterzing (Italy).

At the observation points where two survey marks have been installed, the differences between the displacement at both marks are assessed for investigating potential rotational movements of the respective blocks. Cumulative differences between the displacements in the three axes are evaluated over time and linear models fitted. If the resulting linear trend is statistically significant (5% significance level), a rotational movement is indicated. By applying a local coordinate system, the respective direction of the rotation can be derived. Positive trends represent a rotation in the clockwise horizontal and vertical direction towards south.

The designed low-cost RTK-DGNSS-system (Fig. 2a-c) consists of a base station on stable grounds and a rover located within the active landslide. As GNSS units, a pair of u-blox C94-M8P developer boards were chosen (featuring the NEO-M8P chip), both equipped with a u-blox ANN-MB antenna. The single-frequency system has proven feasible for positional measurements with an accuracy in the order of a few centimetres (Biagi et al. 2016, Poluzzi et al. 2020) and costs less than 400€ (at the time of designing the system). It is capable of utilizing GPS and GLONASS simultaneously. However, for single frequency DGNSSs it is of particular importance that the baseline between base station and rover is considerably small, preventing effects of spatially varying sources of errors (e.g. ionospheric effects including code/carrier divergence and scintillation; Malet et al. 2002, Benoit et al. 2015). Suitable locations on stable grounds as well as on the landslide body were identified, avoiding impact zones of snow avalanches, debris flows and rock fall. The position of the base station was measured with the above referenced DGNSS. The correction data is transferred by a LoRa (long-range) radio module, continuously broadcasting the correction data on a frequency of 433MHz. Utilizing the correction data, the GNSS unit at the rover can obtain precise, fixed-integer positional measurements. A Raspberry Pi zero W is used as controller, scheduling the individual measurements and for data logging. Measurements are conducted with respective Python scripts five times daily over 60 minutes with a sampling rate of 1Hz. Furthermore, an MPU6050 chip, combining a MEMS gyroscope and accelerometer was installed at the rover, capturing the roll and pitch angles of the rover and the sensor temperature. However, the measurements of the accelerometer are biased by temperature changes (e.g. Yang et al. 2017), which – in case of the presented monitoring system – occur due to the seasonal and diurnal variation of air temperature. The recorded inclination in the three axes is compensated accordingly by applying linear models against the recorded sensor temperature. Based on the corrected data, time series of the roll angle $\theta$, pitch angle $\phi$ and tilt angle $\psi$ are computed.

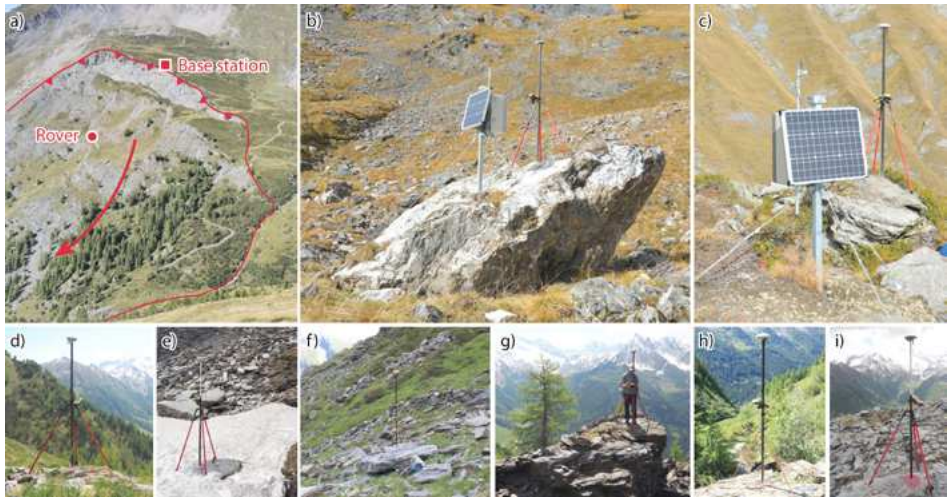


*Figure 2: Overview photo taken from the opposite ridge (a) with the location of the rover (b) and the base station (c). Photos d-i show measurements at the implemented observation points at the point IDs 15, 26, 12, 16, 1 and 13. Photos: J. Branke (a: 2020/09/15; b, c: 2021/10/21), J. Pfeiffer (d, g: 2017/05/30; e, i: 2018/05/25), T. Zieher (f, h: 2016/06/28)*

## RESULTS

The results based on the seasonal and annual monitoring campaigns from 2016/05 to 2021/10 reveal a distinct displacement pattern (Fig. 3a) with total 3D displacements of up to more than 11 metres and landslide velocities exceeding two metres per year (Fig. 3b). The Reissenschuh landslide generally moves eastward and turns towards south-east in the lower part. A scree slope in the southern part between 1900 and 2100 m shows the fastest movement. Along the northern and eastern boundary, the movement rates are distinctly lower. In the season 2018/2019 a markedly higher displacement is evident, likely related to the higher amounts of snow in this particular winter. At the block OP-20, where the rover of the RTK-DGNSS is implemented, a total 3D displacement of 465 ±1.8 cm and a mean velocity of 92.5 cm/yr was observed during the five years' period from 2016/10 to 2021/10. However, the individual displacements assessed at the two survey nails are not in perfect agreement, which could indicate a rotational movement of the block. The continuous displacement time series showing the displacement in the three axes, in 2D and in 3D are presented in Fig. 3c. Most prominent is the east-west component (dX) with in total 91.2 ±0.8 cm, followed by the north-south component (dY) of 29.5 ±0.9 cm and the vertical component (dZ) of 28.2 ±2.1 cm. This results in a total displacement of 95.5 ±1.2 cm in 2D and a displacement of 99.1 ±2.4 cm in 3D, considering the 13 months of monitoring records. The 3D displacement after one year of measurements on 2021/11/09 is 91.5 ±2.4 cm, which is in agreement with the mean annual 3D displacement derived from the periodical DGNSS monitoring at OP-20.

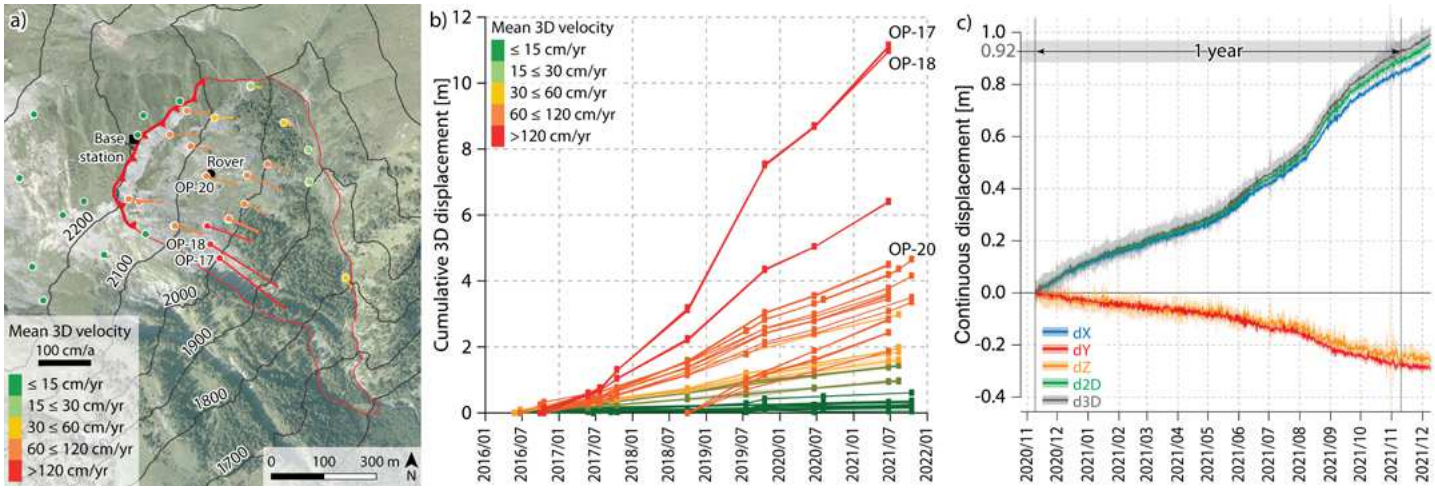


*Figure 3: Results of the periodic DGNSS measurement campaigns at the installed observation points, shown as vectors of mean 3D landslide velocity on the map (a) and as displacement time series with the mean velocity indicated by the colours (b). The continuous displacement time series in (c) are shown for the three axes, as well as in 2D and 3D. The 3D velocity vectors in (a) are shown 100-fold exaggerated.*

The analyses of the differential displacement at the 15 observation points with two survey nails installed revealed a significant 2D rotational movement component at least at four observation points (Fig. 4). The highest differential displacement can be observed at observation point OP-06 (Fig. 4a, e, i), with a total difference of almost -40 cm in east-west direction, indicating a counter-clockwise horizontal rotation. The two blocks OP-17 (Fig. 4b, f, j) and OP-18 (Fig. 4c, g, k), located in the scree slope with the highest movement, both show a minor horizontal clockwise rotation and a statistically significant vertical rotation in the clockwise direction towards south. This means that they slowly topple forward in downslope direction. At OP-20 (Fig. 4d, h, l), no clear horizontal rotational movement of the block can be observed. In

the vertical direction, a minor positive trend is observed, indicating that the block tends to topple forward in downslope direction, where a secondary scarp is currently forming.

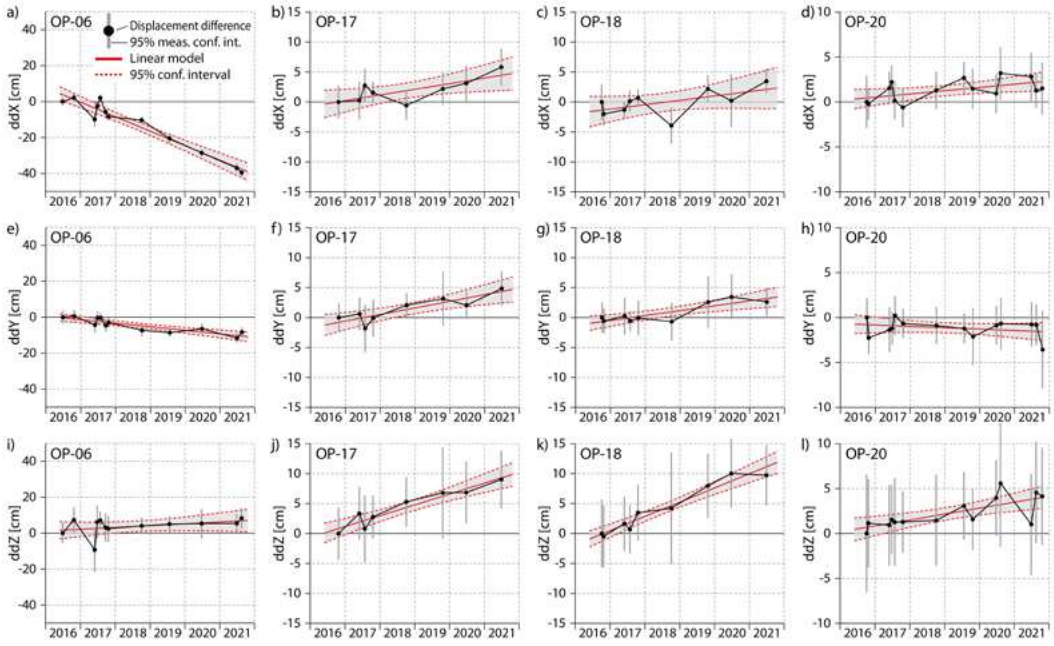


*Figure 4: Cumulative differential displacement between the measurements at the two survey marks of blocks showing distinct trends indicating 2D rotational movements, including OP-06 (a, e, i), OP-17 (b, f, j), OP-18 (c, g, k) and OP-20 (d, h, l). The respective linear trends are shown in red, the 95% CI of the linear model is shaded in grey and delineated by red dashed lines. Positive trends refer to movements in clockwise horizontal and vertical direction towards south. The y-axis is scaled differently for the individual blocks.*

The resulting tilt angle time series recorded by the MEMS accelerometer is shown in Fig. 5. The general direction of the rotational component is a forward tilting towards south-south-east (Fig. 5a). The direction of the rotation diverts from the displacement direction at OP-20 for 51 degrees towards south. However, in the time series of the tilt angle deviation (Fig. 5b), a distinct drop is evident in the beginning of December 2020. This drop coincides with the start of snow accumulation at the Schmirn meteorological station (Fig. 5c). In the course of snow melt, the tilt angle rises again, matching the previously observed value level. Over the year a slightly positive trend of the tilt angle can be observed, indicating a minor rotational movement. In total, the MEMS accelerometer measurements show a tilt of about 0.3°±0.09° RMSE in south-south-east direction, which is in agreement with the rotational movement at OP-20 derived from the periodical DGNSS monitoring (Fig. 4l).

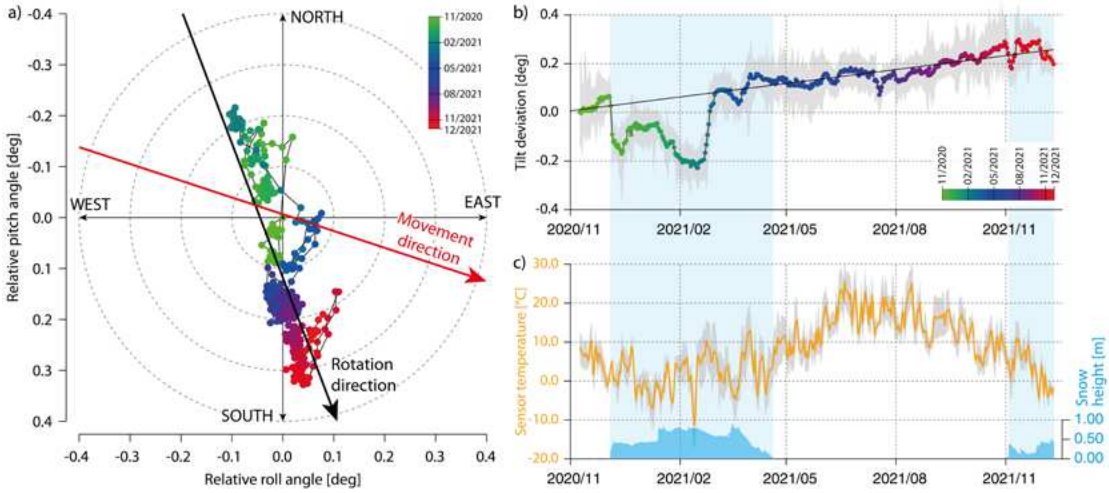


*Figure 5: Tilting of the rover observed by the MEMS accelerometer plotted as horizontal angular deviation (a) and time series, including the 2.5 and 97.5% quantile (shaded grey) (b). The observed daily mean sensor temperature of the accelerometer and its standard deviation (shaded grey) as well as the daily snow depth records of the meteorological station Schmirn are plotted in c). Periods shaded in light blue indicate the presence of a snow cover, causing a bias in the accelerometer records. The colours in a) and b) refer to the date, indicating a forward tilting in south-south-east direction, whereas the movement direction indicated by the red arrow points towards east-south-east.*

## DISCUSSION

The designed low-cost single-band RTK-DGNSS successfully conducted sub-daily positional measurements with a sufficient precision to derive continuous displacement time series at one observation point in the centre of the Reissenschuh landslide. The resulting displacement

is in agreement with the periodical measurements conducted during the presented monitoring period from 2020/11 to 2021/12. The RTK-DGNSS's measurement precision of 2.3 cm (95% CI) in horizontal direction and 4.6 cm (95% CI) in 3D is in agreement with experiments described in other studies using a low-cost DGNSS receiver (Hodgson (2020): 3.7 cm horizontal and 4.2 cm vertical, 95% confidence level). However, a key advantage of the installed RTK base-rover pair is that this system does not require external data during operation. Therefore, the RTK system could operate in remote areas without network coverage.

At the 15 blocks with two survey nails installed, the differences between the respective displacement time series were analysed. At least four blocks show a statistically significant differential displacement in the horizontal and/or vertical direction, indicating not only translational displacement but also a rotational movement component. Three of these four blocks show a forward tilting in the downslope direction, likely caused by the ongoing disintegration and dilatancy of the landslide body. However, based on two survey nails the 3D rotation cannot be readily inferred, because the rotation centre remains unknown. Furthermore, the lower measurement precision in the vertical domain and the related detection limit pose a challenge for analysing such minor rotations.

The relative tilt angle recorded by the MEMS accelerometer shows a slight, but statistically significant increase over time. The resulting measurement precision of ±0.09° RMSE is a bit lower compared to results of lab experiments of other studies (e.g. Cina et al. 2019, precision in the order of ±0.02°), but is still sufficient to detect the block's gradual rotational movement of 0.3° within one year. During periods of snow accumulation, the station slightly tilts towards north, which could be caused by the weight of snow accumulating on top of the box protecting the electronics, mounted on the north-western side of the pole. Also the weight of the snow pack on top of the block could induce a north-westward rotation, depending on the embedment of the block and the location of the pivot point which is unknown. In the winter season 2021/2022 the respective drop of the tilt angle is less distinct than in 2020/2021, while in the beginning snow height is lower in 2021/2022. Therefore, the amount of snow could control the magnitude of the northward tilting of the monitoring system. Overall, however, the rotational movement derived from the tilt angle time series shows minor forward tilting in the south-south-east direction. This is in general agreement with the direction derived from the periodical monitoring time series, also suggesting a forward tilting towards south. However, the direction of the rotation indicated by the MEMS accelerometer is diverting from the movement direction derived from the RTK-DGNSS time series. This difference may be caused by the local changes of topography induced by the landslide's movement. A few meters south of the surveyed block OP-20 the surface shows clear signs of subsidence due to the formation of a new scarp of a faster moving sub-unit of the landslide.

## CONCLUSIONS

This study presents the results of five years of periodical and one year of continuous monitoring of the Reissenschuh landslide's movement based on repeated DGNSS measurements and a permanently installed combined low-cost RTK-DGNSS and MEMS accelerometer. Annual and seasonal measurement campaigns were conducted at 31 implemented observation points using a DNGSS, starting in 2016/05. Since 2020/11, a low-cost RTK-DGNSS continuously monitors the movement one observation point (OP-20), recording sub-daily positions and the tilt angle. The results reveal the long-term displacement of the landslide with varying year-to-year activity, and the landslide dynamics within one year. The displacements derived within the overlapping monitoring period are in good agreement. Furthermore, differential displacement observed at 15 blocks were analysed in terms of their 2D rotational movement component. At OP-20, the resulting rotational movement generally agrees with the continuous tilt angle time series, both indicating a minor forward toppling in downslope direction.
The combined low-cost RTK-DGNSS and MEMS accelerometer proved feasible for monitoring the movement of the Reissenschuh landslide and features a sufficient measurement precision. The system is based on standard components and open-source software with material costs of about 2000€ in total for both stations and could be replicated in comparable case studies easily. The core system does not rely on an external communication network (e.g. GSM, Internet) and can be implemented in remote areas without network coverage.

## ACKNOWLEDGEMENTS

We thank an anonymous reviewer for the helpful feedback. This study was supported by the Tyrolean Science Fund, project EMOD-SLAP.

## REFERENCES

*Benoit L., Briole P., Martin O., Thom C., Malet J.-P., Ulrich P. (2015). Monitoring landslide displacements with the Geocube wireless network of low-cost GPS, Engineering Geology 195: 111-121.*

*Biagi L., Grec F. C., Negretti M. (2016). Low-Cost GNSS Receivers for Local Monitoring: Experimental Simulation, and Analysis of Displacements, Sensors 16(12): 2140.*

*Cina A., Manzino A. M., Bendea I. H. (2019). Improving GNSS Landslide Monitoring with the Use of Low-Cost MEMS Accelerometers, Applied Sciences 9(23): 5075.*

*Gili J. A., Corominas J., Rius J. (2000). Using Global Positioning System techniques in landslide monitoring, Engineering Geology 55(3): 167-192.*

*Haque U., da Silva P. F., Devoli G., Pilz J., Zhao B., Khaloua A., Wilopo W., Andersen P., Lu P., Lee J., Yamamoto T., Keellings D., Wu J.-H., Glass G. E. (2019). The human cost of global warming: Deadly landslides and their triggers (1995–2014), Science of The Total Environment 682: 673-684.*

*Heunecke O., Glabsch J., Schuhbäck S. (2011). Landslide monitoring using low cost GNSS equipment n experiences from two alpine testing sites, Journal of civil engineering and architecture 5(8): 661-669.*

*Hodgson M. E. (2020). On the accuracy of low-cost dual-frequency GNSS network receivers and reference data, GIScience & Remote Sensing 57(7): 907-923.*

*Lapadat A. M., Tiberius C. C. J. M., Teunissen P. J. G. (2021). Experimental Evaluation of Smartphone Accelerometer and Low-Cost Dual Frequency GNSS Sensors for Deformation Monitoring, Sensors 21(23): 7946.*

*Malet J.-P., Maquaire O., Calais E. (2002). The use of Global Positioning System techniques for the continuous monitoring of landslides: application to the Super-Sauze earthflow (Alpes-de-Haute-Provence, France), Geomorphology 43(1): 33-54.*

*Petley D. (2012). Global patterns of loss of life from landslides, Geology 40(10): 927-930.*

*Pfeiffer J., Zieher T., Bremer M., Wichmann V., Rutzinger M. (2018). Derivation of Three-Dimensional Displacement Vectors from Multi-Temporal Long-Range Terrestrial Laser Scanning at the Reissenschuh Landslide (Tyrol, Austria), Remote Sensing 10(11): 1688.*

*Poluzzi L., Tavasci L., Corsini F., Barbarella M., Gandolfi S. (2020). Low-cost GNSS sensors for monitoring applications, Applied Geomatics 12(1): 35-44.*

*Rockenschaub M., Kolenprat B., Nowotny A. (2003) Das westliche Tauernfenster, in Geologische Bundesanstalt - Arbeitstagung 2003: Blatt 148 Brenner, 7-38.*

*Šegina E., Peternel T., Urbancic T., Realini E., Zupan M., Jež J., Caldera S., Gatti A., Tagliaferro G., Consoli A., González J. R., Auflic M. J. (2020). Monitoring Surface Displacement of a Deep-Seated Landslide by a Low-Cost and near Real-Time GNSS System, Remote Sensing 12(20): 3375.*

*Teunissen P. J. G., Montenbruck O. (2017). Springer handbook of global navigation satellite systems, Vol. 10, Springer.*

*Tu R., Wang R., Ge M., Walter T. R., Ramatschi M., Milkereit C., Bindi D., Dahm T. (2013). Cost-effective monitoring of ground motion related to earthquakes, landslides, or volcanic activity by joint use of a single-frequency GPS and a MEMS accelerometer, Geophysical Research Letters 40(15): 3825-3829.*

*Yang D., Woo J.-K., Lee S., Mitchell J., Challoner A. D., Najafi K. (2017). A Micro Oven-Control System for Inertial Sensors, Journal of Microelectromechanical Systems 26(3): 507-518.*